

MOLECULAR AND SYNAPTIC MECHANISMS

Loss of the calcium channel β_4 subunit impairs parallel fibre volley and Purkinje cell firing in cerebellum of adult ataxic mice

Bruno Benedetti, Ariane Benedetti and Bernhard E. Flucher

Department of Physiology and Medical Physics, Medical University of Innsbruck, Schöpfstraße 41, Innsbruck, A-6020, Austria

Keywords: ataxia, cerebellar cortex, development, electrophysiology, neuron

Edited by László Acsády

Received 18 January 2016, revised 17 March 2016, accepted 18 March 2016

Abstract

The auxiliary voltage-gated calcium channel subunit β_4 supports targeting of calcium channels to the cell membrane, modulates ionic currents and promotes synaptic release in the central nervous system. β_4 is abundant in cerebellum and its loss causes ataxia. However, the type of calcium channels and cerebellar functions affected by the loss of β_4 are currently unknown. We therefore studied the structure and function of Purkinje cells in acute cerebellar slices of the $\beta_4^{-/-}$ ataxic (*lethargic*) mouse, finding that loss of β_4 affected Purkinje cell input, morphology and pacemaker activity. In adult *lethargic* cerebellum evoked postsynaptic currents from parallel fibres were depressed, while paired-pulse facilitation and spontaneous synaptic currents were unaffected. Because climbing fibre input was spared, the parallel fibre/climbing fibre input ratio was reduced. The dendritic arbor of adult *lethargic* Purkinje cells displayed fewer and shorter dendrites, but a normal spine density. Accordingly, the width of the molecular and granular layers was reduced. These defects recapitulate the impaired cerebellar maturation observed upon $\text{Ca}_v2.1$ ataxic mutations. However, unlike $\text{Ca}_v2.1$ mutations, *lethargic* Purkinje cells also displayed a striking decrease in pacemaker firing frequency, without loss of firing regularity. All these deficiencies appear in late development, indicating the importance of β_4 for the normal differentiation and function of mature Purkinje cells networks. The observed reduction of the parallel fibre input, the altered parallel fibre/climbing fibre ratio and the reduced Purkinje cell output can contribute to the severe motor impairment caused by the loss of the calcium channel β_4 subunit in *lethargic* mice.

Introduction

In cerebellum, presynaptic P/Q-type calcium channels are made up of the pore-forming $\text{Ca}_v2.1$ α_1 subunit and auxiliary subunits, among which β_4 and $\alpha_2\delta-2$ are the most highly represented (Buraei & Yang, 2010; Schlick *et al.*, 2010). Consistent with their joint function in cerebellar neurons, mutation of any one of these calcium channel subunits in mice and humans leads to similar forms of ataxia and epilepsy (Dung & Swigart, 1971; Fletcher *et al.*, 1996; Burgess *et al.*, 1997; Escayg *et al.*, 2000; Barclay *et al.*, 2001; Brodbeck *et al.*, 2002; Khan & Jinnah, 2002; Pietrobon, 2005; Dolphin, 2012; Noebels, 2012). Although it is well established that dysfunctions of $\text{Ca}_v2.1$ or $\alpha_2\delta-2$ affect the morphology, synaptic input and pacemaker activity of cerebellar Purkinje neurons (Zwingman *et al.*, 2001; Matsushita *et al.*, 2002; Kodama *et al.*, 2006; Walter *et al.*, 2006; Lonchamp *et al.*, 2009), the specific cerebellar functions of the β_4 subunit and their causal link to the ataxic phenotype in β_4 loss-of-function mutations remain elusive.

Calcium channel β subunits associate with Ca_v1 and Ca_v2 α_1 subunits. They modulate their current properties and are important for proper membrane expression and subcellular targeting of the channels (Buraei & Yang, 2010; Etemad *et al.*, 2014; Campiglio & Flucher, 2015). Consequently β_4 subunits are important for calcium-induced neurotransmitter release at synaptic terminals of central nervous system (CNS) neurons (Caddick *et al.*, 1999; Lin *et al.*, 1999; Wittemann *et al.*, 2000). Furthermore, new channel-independent functions of β_4 in gene transcription regulation have recently emerged, suggesting potential roles of this protein in regulation of neuronal development and physiology (Tadmouri *et al.*, 2012; Etemad *et al.*, 2014). Previous studies in the ataxic $\beta_4^{-/-}$ mouse model (*lethargic*) suggested that the function of β_4 in CNS neurons might be redundant and that the lack of β_4 is largely compensated for by increased expression of other β isoforms (McEnery *et al.*, 1998). This notion is consistent with the observation that calcium currents in Purkinje cell (PC) somas are unaffected by loss of β_4 (Burgess & Noebels, 1999a). However, a redundancy of β_4 is at odds with the prominent motor impairment in *lethargic* mice (Burgess *et al.*, 1997; Khan & Jinnah, 2002) and the functional compensation, which occurs at the PC soma (Burgess *et al.*, 1999), might not

Correspondence: Dr Bruno Benedetti and Dr Bernhard E. Flucher, as above.
E-mails: bruno.benedetti@i-med.ac.at and bernhard.e.flucher@i-med.ac.at

necessarily extend to dendrites, axons and synapses (Witte mann *et al.*, 2000; Obermair *et al.*, 2010; Etemad *et al.*, 2014).

Here we applied electrophysiological recordings from PCs in acute cerebellar slices of $\beta_4^{-/-}$ *lethargic* mice to test the hypothesis that the calcium channel β_4 subunit is necessary for normal function of cerebellar cortex networks, where physiological defects upon loss of β_4 may contribute to the ataxic phenotype in *lethargic* mice. We reasoned that, because β_4 is an essential subunit of P/Q-type calcium channels, the deficiencies in PC networks in *lethargic* mice will resemble those previously reported in $\text{Ca}_v2.1$ mutant mice, unless compensated for by redundant β functions. On the other hand, β_4 -specific defects will expose essential roles of β_4 in other Ca_v isoforms and channel-independent functions of β_4 in the development of cerebellar cortex networks.

Materials and methods

Animal handling

All animal procedures were performed according to the guidelines of ethical approval by the European Parliament Directive (Council Directive 2010/63EU and Council of 22 September 2010) for the protection of animal used for scientific purposes and were approved by the Austrian Ministry BMWF, TWG 2012. Animals were kindly provided by the laboratory of Professor V. Flockerzi, Universität Saarland (Germany). For all animal experiments, the 3Rs system was followed (replacement, reduction and refinement). Experiments were carried out on animals of either sex. To ease the access to food and further promote the fitness and comfort of *lethargic* mice, dry food pellets and hydrating gel was placed on the cage floor and provided *ad libitum*. All mice were bred at least for ten generations into 129/SvJ inbred background. *Wildtype* and *lethargic* ($\beta_4^{-/-}$) mice were obtained by homozygous mating. The numbers of animals used for the experiments were: 16 juvenile [postnatal day (P)07–P20] *wildtype*, 20 juvenile *lethargic*, 34 adult (P35–P65) *wildtype* and 20 adult *lethargic* mice.

Electrophysiology

After killing the mice by cervical dislocation and after decapitation, scalp and skull bones were gently removed with the help of fine scissors and tweezers. After this, the mouse cerebellum was acutely dissected and immediately chilled ($\sim 0^\circ\text{C}$) in artificial cerebrospinal fluid containing (in mm): NaCl, 125; NaHCO_3 , 26; glucose, 10; KCl, 2.5; NaH_2PO_4 , 1.25; CaCl_2 , 2; MgCl_2 , 1; pH was adjusted to 7.4 with a saturating carbogen mix (95/5% CO_2/O_2). Parasagittal cerebellar slices were cut along the vermis, with a vibratome (Leica VT1200S). After dissection, slices were stored in artificial cerebrospinal fluid at $21.5\text{--}22.5^\circ\text{C}$ (room temperature) for up to 5 h.

Recordings were obtained from visually identified PCs from the anterior lobe, mostly within lobules III and IV. Electrophysiological data were acquired with an Axon 900A amplifier and the software pCLAMP (Axon Instruments, Union City, CA, USA); sampling rate was 20 kHz. Traces were filtered at 1–4 kHz and analysed with Origin, Microsoft Excel and GRAPHPAD-PRISM. Series resistances (R_s) were typically about 10 M Ω . R_s compensation was applied at 60–70%. Recordings with R_s drift $> 10\%$ were discarded. The internal pipette solution contained (in mm): K-gluconate, 132; EGTA/KOH, 1; MgCl_2 , 2; NaCl, 2; HEPES/KOH, 10; Mg-ATP, 2; GTP, 0.5; pH was adjusted to 7.2 (Lonchamp *et al.*, 2009). Pipette resistance was about 2 M Ω for whole-cell measurements and 3–7 M Ω for cell-attached recordings. Parallel fibre (PF) volleys were evoked by unipolar stimulation

electrode (glass pipette of about 1 M Ω) in the molecular layer beneath the pial surface. Climbing fibre (CF) responses were evoked by similar stimulation in the granular layer. In the representative recordings of evoked synaptic responses, the stimulation artefacts were removed for clarity of representation. The optimal age range for electrophysiological recording was determined after preliminary excitatory postsynaptic current (ePSC) and inhibitory postsynaptic current (iPSC) measurement between P06 and P20, where the largest increase in PSC frequency occurred before P12 (data not shown). ePSC and iPSC on young mice were sampled at room temperature from mice between P12 and P20, with the same distribution between $\beta_4^{+/+}$ and $\beta_4^{-/-}$ (14.5 ± 1.0 and 15.0 ± 0.9 , respectively). Pacemaker firing was measured at $34\text{--}36^\circ\text{C}$. Action potential frequency in young mice was determined in cell-attached experiments at P14–P15. Action potential frequency in adult mice was recorded between postnatal weeks 5 and 8 ($P43 \pm 1$ for $\beta_4^{+/+}$ and $P44 \pm 1$ for $\beta_4^{-/-}$); cells from the same mice were also used for morphological analysis. In adult populations no correlation existed between ages and firing frequency ($R = 0.3$, $P = 0.5$ for $\beta_4^{+/+}$ and $R = -0.6$, $P = 0.1$ for $\beta_4^{-/-}$). Evoked postsynaptic currents were recorded at P15 and P55–P65 (P60). Drugs were applied at the following concentrations (mM): (\pm)-*trans*-1-amino-1,3-dicarboxycyclopentane (*trans*-ACPD; Tocris, Bristol, UK) 0.05; SR 95531 hydrobromide (gabazine; Tocris) 0.01; and 6,7 dinitroquinoxaline-2,3-dione (DNQX; Tocris) 0.01, DL-AP-5 (AP-5; Tocris) 0.05.

Morphological analysis

During whole-cell patch clamp recordings, Purkinje neurons were dialysed with biocytin via patch-pipette (Benedetti *et al.*, 2011). After 10–20 min the pipette was gently retracted, slices were transferred to 4% sucrose/paraformaldehyde in 0.1 M phosphate buffer, and stored at 4°C for 24–96 h before staining. Then, slices were thoroughly rinsed in phosphate-buffered saline, incubated for 1 h in 0.2% Triton-X100 at room temperature, rinsed and again with phosphate buffer. To block endogenous biotin, slices were treated with the Endogenous Biotin-Blocking Kit (Molecular Probes, Carlsbad, CA, USA). Streptavidin conjugated with Alexa Fluor 568 (Molecular Probes) was added (1:1000 in phosphate-buffered saline) and incubated overnight at 4°C with shaking. Finally, slices were thoroughly rinsed in phosphate buffer and mounted with Vectashield (Vector Laboratories, Burlingame, CA, USA). Labelled neurons were imaged using a confocal microscope (SP5; Leica, Wetzlar, Germany) using a 20 \times air objective and LEICA LAS AF software. For morphological analysis, vertical projections of z-stacks were processed with the software LAS AF (Leica) and IMAGE J. For Scholl analysis, intersections were counted between dendritic branches and concentric circles, starting at 6 μm from the cell soma and at radial increments of 3 μm , up to 250 μm (maximal radial dendrite extension). Dendritic tracking was performed with the 'Neuron J' plugin to IMAGE J (courtesy of Dr Erik Meijering, Erasmus University Medical Center Rotterdam). Counting of synaptic spines was performed on higher-magnification scans (63 \times glycerol objective) from non-overlapping portions of proximal ($< 100 \mu\text{m}$ from soma) or distal ($> 100 \mu\text{m}$ from soma) dendrites. The number of spines was then normalized for the length of the analysed dendrite.

Data analysis and statistics

Statistical analysis was performed with the software GRAPHPAD-PRISM 5.03. Statistical significance in the comparison among groups was determined as follows. (i) Normality of data distribution was determined for each group with the Kolmogorov–Smirnov test. (ii) In

case of a normal distribution, a *t*-test or analysis of variance (ANOVA) + Bonferroni test were used for comparison between, respectively, two or multiple groups. (iib) In case of a non-normal distribution, Mann–Whitney test or Kruskal–Wallis + Dunn’s test were used for comparison between, respectively, two or multiple groups (see Figs 5 and 6). (iii). Two-way ANOVA was used to compare differences in PF–PC PSC in the presence or absence of β_4 at each stimulation intensity (see Fig. 2). The type of test employed to analyse each set of data is specified in the figures and tables. Bar graphs represent mean \pm standard error of the mean (SEM). Scatter dot plots represent single data points. Plots in which symbols are connected by lines (Figs 1H and I, and 3F) represent paired sets of data. Box plots (Fig. 2) represent mean, interquartile range and 5–95% of range. Numerical *P* values are reported in the tables, where *F* and *P* values are reported for repeated measurements (*F*; *P*). Significance is indicated as: **P* < 0.05, ***P* < 0.001, ****P* < 0.0001. The number of independent samples (different cells) is reported in parentheses in the figures and tables. For each type of experiment, measurements were carried out on three or more $\beta_4^{+/+}$ and three or more $\beta_4^{-/-}$ mice, except for the measurements of pacemaker firing in the presence of DNQX/gabazine (Fig. 5) which were carried out on two animals.

Results

Loss of β_4 does not reduce the spontaneous synaptic input of Purkinje neurons

The β_4 subunit is known to support $\text{Ca}_v2.1$ calcium channel activity and thus promotes synaptic transmission in CNS thalamic neurons and in cultured hippocampal neurons (Caddick *et al.*, 1999;

Wittmann *et al.*, 2000). Therefore, loss of β_4 in *lethargic* ($\beta_4^{-/-}$) mice is expected to severely affect the activity of $\text{Ca}_v2.1$ in cerebellar neurotransmission (Lonchamp *et al.*, 2009; Galliano *et al.*, 2013). To test this possibility we performed patch clamp recordings of ePSC and iPSC in PCs of acute cerebellar slices. In the whole-cell configuration the membrane potential of PCs was held at -40 mV in 1-week-old mice (P07), or at -70 mV in 2-week-old mice (P15). At P07 (Fig. 1A) postsynaptic currents principally comprised ePSCs, while iPSCs were very rare (Fig. 1B and C). At P15 (Fig. 1D) ePSCs and iPSCs occurred at increased frequency (Fig. 1E and F; *P* > 0.04). Importantly, at both ages we found no difference in the frequency of ePSCs or iPSCs between *lethargic* and age-matched control cerebellar slices (Table 1). Current amplitude was also not impaired by the lack of β_4 ; while the ePSC amplitude was slightly increased in *lethargic* mice (Table 1), the iPSC amplitude was not changed.

Because excitatory input from granule cells to PCs is subject to tonic GABAergic inhibition (Hamann *et al.*, 2002), we wondered whether this inhibitory activity could have masked differences in excitatory synaptic activity. Therefore, in a subset of experiments ePSCs were recorded in the presence of the selective GABA receptor blocker gabazine (Fig. 1G). In cerebellar slices from animals older than 12 days, gabazine (10 μM) completely blocked the iPSCs and concomitantly led to a significant increase of ePSC frequency (paired *t*-test; *P* = 0.03, $\beta_4^{+/+}$; *P* = 0.01, $\beta_4^{-/-}$). Younger cerebellar slices (< P12) were not affected (*P* = 0.2, $\beta_4^{+/+}$; *P* = 0.4, $\beta_4^{-/-}$). Notably, the effect of gabazine was not different between wildtype (Fig. 1H) and *lethargic* neurons (Fig. 1I). Together these data demonstrate that loss of β_4 does not impair the spontaneous synaptic transmission onto PCs. Considering the importance of P/Q-type

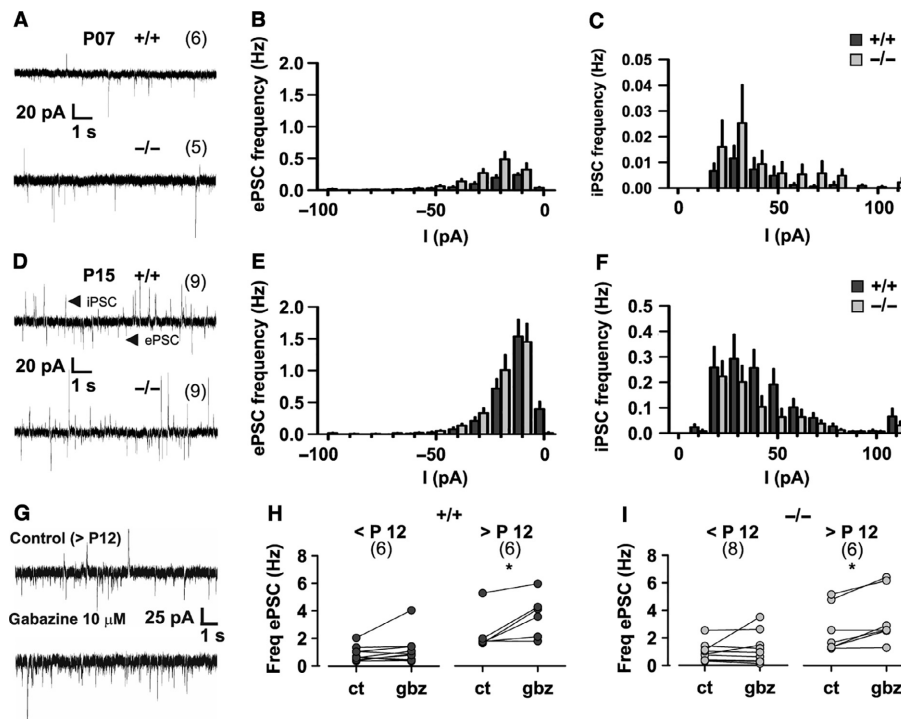


FIG. 1. Spontaneous excitatory and inhibitory postsynaptic currents (ePSCs and iPSCs) in young Purkinje neurons from wildtype (+/+) and *lethargic* (–/–) mice. (A, D) Representative recordings from P07 and P15 mice show ePSCs and iPSCs as inward and outward current spikes, respectively. (B, C, E, F) Graphs depicting ePSC and iPSC amplitude and frequency in P07 (B, C) and P15 mice (E, F). (G) iPSCs and ePSCs in control conditions, and in the presence of gabazine; note the absence of iPSCs after gabazine application. (H, I) Mean ePSC frequency in paired recordings before and after gabazine application in +/+ (H) and –/– (I) mice. Note the significant increase in ePSC frequency in both +/+ and –/– mice after P12. Bar graphs indicate mean \pm SEM; ANOVA tests were used for comparison of amplitude and frequency as detailed in Table 1. A paired *t*-test was used in H and I; **P* < 0.05. Numbers of independent samples are indicated in parentheses in the figure.

TABLE 1. Postsynaptic current (PSC) frequency and amplitude

	Frequency (Hz)		<i>n</i>	Amplitude (pA)			Postnatal days
	ePSC	iPSC		ePSC	iPSC	<i>n</i>	
$+/+$ P07	0.8 ± 0.2	0.15 ± 0.07	6; 6	25 ± 1	29 ± 4	6; 4	7.0 ± 0.0
$-/-$ P07	0.6 ± 0.1	0.13 ± 0.07	5; 5	35 ± 2	54 ± 17	5; 3	6.8 ± 0.2
<i>P</i> *	0.4	0.9		0.009	0.15		
ANOVA: <i>F</i> ; <i>P</i>	–	–		19.73; < 0.0001	2.1; 0.1		
Bonferroni	–	–		< 0.001	–		
$+/+$ P15	3.0 ± 0.6	1.3 ± 0.4	9; 9	18 ± 1	49 ± 6	9; 9	15.0 ± 0.8
$-/-$ P15	3.2 ± 0.5	0.8 ± 0.2	9; 9	25 ± 1	35 ± 5	9; 9	16.0 ± 0.9
<i>P</i> *	1.0	0.4		0.0005	0.1		
ANOVA: <i>F</i> ; <i>P</i>	–	–		19.73; < 0.0001	2.1; 0.1		
Bonferroni	–	–		< 0.05	–		

Mean ± SEM are reported. **P* values refer to unpaired *t*-test. ANOVA (*F*; *P*) values refer to multiple comparisons between groups of different age, and Bonferroni post-test (*P*) amongst the same data. –, not tested; *n*, number of samples.

calcium channels for presynaptic function, this suggests that the lack of β_4 in cerebellar synapses of *lethargic* mice may be compensated for by other β isoforms, as previously suggested (McEnery *et al.*, 1998; Burgess *et al.*, 1999).

Loss of β_4 in adult *lethargic* mice specifically affects PF volley but not paired-pulse facilitation (PPF)

Although β_4 loss did not impair spontaneous synaptic activity, it might affect PF input via postsynaptic mechanisms, similar to what was previously observed in $\text{Ca}_v2.1$ mutations (Matsushita *et al.*, 2002; Kodama *et al.*, 2006). We therefore measured postsynaptic currents evoked by synchronous synaptic release from PFs (PF–PC PSCs). Electrical pulses increasing from 5 to 30 μA were locally delivered in the molecular layer. In both young and adult PCs these stimuli triggered PF–PC PSCs of increasing amplitudes (Fig. 2A and C; Table 2). In cerebellum of young *lethargic* mice the amplitudes of the evoked PF–PC PSCs were comparable to those recorded in wildtype controls. As PPF is a measure of presynaptic calcium signalling and regulation of release probability, we also recorded PSCs in response to two consecutive stimuli of equal strength (Fig. 2B). In young wildtype and *lethargic* mice the paired-pulse ratios (PPRs) of PF–PC synapses were not significantly different. Thus, in young mice the function of PF–PC synapses and total synaptic input from PFs is apparently not affected by the lack of the calcium channel β_4 subunit.

In contrast, evoked PF–PC PSCs were significantly decreased in adult *lethargic* cerebellum (Fig. 2C). Under the assumption that axonal excitability, axonal density and probability of PF–PC connection are not altered, changes in the PF–PC PSC in *lethargic* mice would imply altered synaptic transmission. Here PSC amplitudes evoked by 30- μA pulses were about half the size of PSCs in age-matched wildtype controls ($-/-$, 0.5 ± 0.1 nA; $+/+$, 0.9 ± 0.1 nA; *P* = 0.03). Nevertheless, PPRs in adult *lethargic* mice were still unaltered (Fig. 2D; *P* = 0.4). Thus, the loss of β_4 dramatically decreased the total synaptic input from PFs in adult but not in juvenile *lethargic* mice. However, the unaltered release probability indicates that this dysfunction does not arise from an impeded presynaptic function in PF–PC synapses.

Because these results suggested a postsynaptic mechanism affecting excitatory neurotransmission in PCs of adult *lethargic* mice, we next examined synaptic input from CFs. Electrical stimuli in the granular layer typically evoked large all-or-none postsynaptic currents with effective stimulation thresholds between 10 and 25 μA

(Fig. 2E and F). In the cerebellum of wildtype and *lethargic* mice, the amplitudes of CF–PC PSCs were not significantly different from each other (Fig. 2F; Table 2, *P* = 0.9), equal to 10.5 ± 2.1 and 10.8 ± 2.0 nA, respectively, at a stimulus intensity of 30 μA . This indicates that, contrary to PF input, β_4 is not critically involved in shaping the synaptic input of CFs to PCs.

In our whole-cell recordings, we noticed that the cell capacitance of adult $\beta_4^{-/-}$ PCs was significantly smaller than that of adult $\beta_4^{+/+}$ neurons ($-/-$, 925 ± 42 pF; $+/+$, 1643 ± 70 pF; *P* < 0.0001; Fig. 2G). No difference was detected at P15 (*P* = 0.8) and in younger mice (P07, P10). When PF–PC PSCs were normalized to the capacitance of each respective neuron, the resulting current densities were not significantly different (*P* = 0.7) between *lethargic* and wildtype mice. Similarly, the integrals of PF–PC PSC/whole cell capacitance of both genotypes were not significantly different (*P* = 0.5; Fig. 2H; Table 2). Thus, in *lethargic* mice the reduction of the PF–PC input matches the decrease in PC size. Integrals of CF–PC PSCs instead did not correspond to the decreased PC cell capacitance. Consequently, the density of CF–PC PSCs was significantly increased in the smaller *lethargic* PCs compared to wildtype controls (Fig. 2H; *P* < 0.01), and the resulting CF–PC PSC/PF–PC PSC ratio was smaller in *lethargic* mice. Furthermore, this decrease in PC capacitance and the associated decrease of PF–PC input in adult *lethargic* mice suggests that the loss of the calcium channel β_4 subunit affects the late differentiation of the dendritic compartment of PCs.

Loss of β_4 affects PC dendritic morphology in adult mice

To further examine the differentiation of PCs dendritic compartment, we analysed the dendritic shape and length in wildtype and *lethargic* PCs. The neurons were dialysed with biocytin via the patch pipette during whole-cell recordings in acute cerebellar slices. Streptavidin staining of the labelled cells revealed the structure of the complete dendritic arbor (Fig. 3A). Using Scholl analysis we quantified dendritic branching and extension. The overall appearance, size and branching of juvenile *lethargic* PC dendrites was comparable to that of controls (Fig. 3A and B; *F* = 0.4, *P* = 0.5, *n*: $+/+$ = 18, *n*: $-/-$ = 11). By contrast, in adult *lethargic* mice dendritic branches were fewer and shorter than in age-matched wildtype controls (Fig. 3B and C; *F* = 22.3, *P* = 0.0001 *n*: $+/+$ = 10, *n*: $-/-$ = 11). However, weeping-willow-like structures (Zwingman *et al.*, 2001), or missing portions of the dendritic arbor (Kodama *et al.*, 2006) were not observed. Dendrites were also counted within three

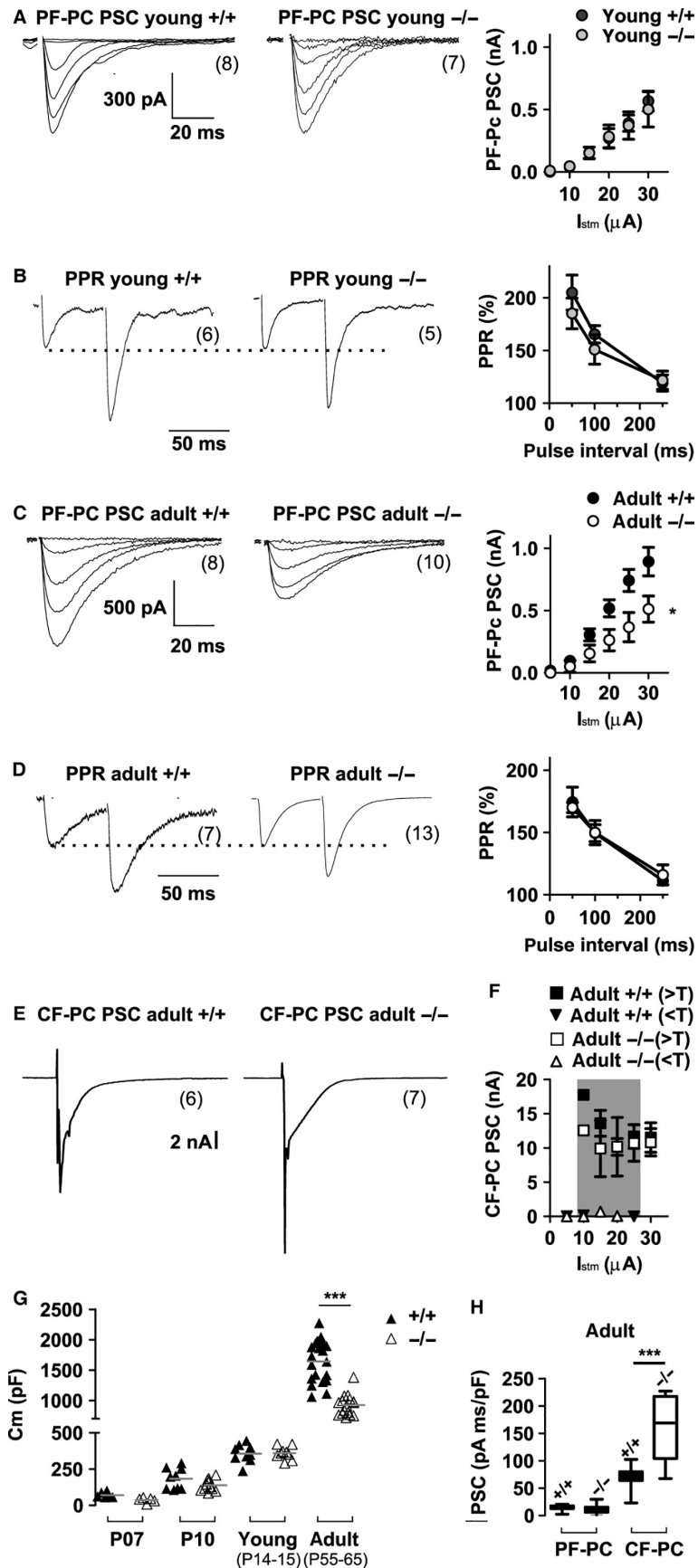


FIG. 2. Evoked postsynaptic currents (PSCs) and paired pulse facilitation in cerebellar Purkinje neurons upon stimulation of parallel fibres and climbing fibres in wildtype (+/+) and *lethargic* (-/-) mice. (A–D) Representative PF volley recordings in juvenile (A, B) and adult (C, D) mice; * $P < 0.05$; two-way ANOVA. (A, C) PSC amplitude in responses to increasing stimulus intensity displays a significantly higher amplitude in adult +/+ compared to -/- mice (c). (B, D) PPF upon repetitive PF stimulation shows that the PPRs are not different in *lethargic* mice compared to age-matched controls (mean \pm SEM). (E) Representative PSCs upon CF stimulation. (F) CF–PC PSC all-or-none responses display constant amplitude at increasing stimulus intensities above effective threshold ($> T$, squares) and below threshold ($< T$, triangles). (G) Differences in whole cell capacitance (C_m) in adult PCs reveals a significantly decreased PC size in -/- mice. (H) Integral of PF–PC and CF–PC PSCs normalized to whole cell capacitance demonstrates that relative to cell size current density of PF–PC is identical in genotypes, but CF–PC current density is significantly increased in -/- mice. Box-plots show mean, inter-quartile distribution and 10–90% of the data range. ‘Young’ mice were P14–P15, while ‘adult’ mice were P55–P65. Differences between PF–PC PSCs were measured at any stimulation intensity with two-way ANOVA test; other differences between multiple populations (G, H) were measured with one-way ANOVA test followed by Bonferroni post-test as detailed in Table 2. * $P < 0.05$; *** $P < 0.0001$. Numbers of independent samples are indicated in parentheses in the figure.

TABLE 2. PF–PC PSC amplitude, paired pulse ratios and CF–PC PSC amplitude; see also Fig. 2

	PF–PC PSC (STM = 30 μ A)			CF–PC PSC		
	nA	nA/pF	\int PSC/ C_m (pA.ms)/pF	PF–PC PPR	nA	\int PSC/ C_m (pA.ms)/pF
+/+ young (P14–15)	0.6 \pm 0.1 ($n = 8$)			209 \pm 21 ($n = 7$)		
-/- young (P14–15)	0.6 \pm 0.1 ($n = 6$)			185 \pm 14 ($n = 5$)		
P^*	0.7			0.7		
+/+ adult (P55–65)	0.9 \pm 0.1 ($n = 8$)	0.54 \pm 0.05 ($n = 8$)	15 \pm 2 ($n = 8$)	182 \pm 10 ($n = 7$)	11.5 \pm 2.2 ($n = 6$)	69 \pm 9 ($n = 6$)
-/- adult (P55–65)	0.5 \pm 0.1 ($n = 10$)	0.61 \pm 0.15 ($n = 10$)	12 \pm 3 ($n = 10$)	170 \pm 4 ($n = 13$)	10.8 \pm 2.0 ($n = 7$)	158 \pm 24 ($n = 7$)
P^*	0.03	0.7	0.5	0.4	0.9	0.009
ANOVA: F ; P	–	–	34; < 0.0001	–	–	34; < 0.0001
Bonferroni	–	–	ns	–	–	< 0.0001
A-2 (S): F ; P	5.3; 0.03	–	–	–	–	–
A-2 (T): F ; P	58; < 0.001	–	–	–	–	–

Mean \pm SEM are reported. * P values refer to unpaired t -test. ANOVA (F ; P) values refer to multiple comparison between all evoked responses (PF–PC PSCs and CF–PC PSCs) normalized for cell capacitance in adult mice followed by Bonferroni post-test. ns, not significant; –, not tested. Two-way ANOVA (F ; P) analyses the differences between PF–PC PSC amplitudes in the presence or absence of β_4 (A2-S) at each stimulation intensity (A2-T; intensity = 5–30 μ A).

concentric annular areas centred at the soma (proximal = 0–70 μ m; medial = 70–120 μ m; distal = 120–200 μ m). The greatest differences occurred in the distal ($P < 0.0001$) and medial circle ($P = 0.01$). In the proximal circle, the number of dendrites was comparable in cerebella of *lethargic* and wildtype mice ($P = 0.1$). Total dendrite lengths were equal in young *lethargic* and wildtype mice (-/-, 3.6 \pm 0.2 mm; +/+, 3.8 \pm 0.4 mm; $P = 0.7$; Fig. 3D). In adults, however, *lethargic* dendrites were significantly shorter than in control PCs (-/-, 3.1 \pm 0.1 mm; +/+, 5.4 \pm 0.1 mm; $P < 0.0001$; unpaired t -test). In agreement with the electrophysiological data described above, these results reveal a severely retarded differentiation of distal PC dendrites in the absence of β_4 .

If this deficiency in the PC dendrites in *lethargic* cerebellum arises from a diminished number of PFs and sparser synaptic contacts, a decrease in spine density would also be expected (Oda *et al.*, 2011). Therefore, synaptic spines were counted in non-overlapping dendritic segments of wildtype and *lethargic* PCs in proximal and distal dendrites (Fig. 3E). Spine density in $\beta_4^{+/+}$ and $\beta_4^{-/-}$ neurons was comparable in proximal and distal dendrites (proximal: +/+, 2.3 \pm 0.2/ μ m; -/-, to 2.1/ μ m; $P = 0.6$; distal: +/+, 2.3 \pm 0.1/ μ m; -/-, 2.3 \pm 0.2/ μ m; $P = 0.8$. Fig. 3F). Also the ratios of spine density in proximal to distal spines were not significantly different in the two genotypes (+/+, 1.01 \pm 0.09; -/-, 0.95 \pm 0.08; $P = 0.6$. Fig. 3G). Evidently, although the size of the distal dendritic arbor is substantially decreased in *lethargic* PCs, the density of synaptic spines on the remaining dendritic branches is unchanged.

The reduced size of the dendritic arbor is expected to result in a reduced width of the molecular layer. Furthermore, a decreased synaptic input from PFs may originate from a smaller number of granule cells. To examine these possibilities, we measured the

widths of the molecular and granular cell layers in wildtype and *lethargic* acute cerebellar slices (Fig. 3H). Indeed, the widths of both the molecular and the granular cell layers were significantly reduced in *lethargic* mice (molecular layer: +/+, 240 \pm 6 μ m; -/-, 200 \pm 6 μ m; granular layer: +/+, 200 \pm 4 μ m; -/-, 160 \pm 4 μ m; $P < 0.0001$; Fig. 3I). Thus, the lack of β_4 not only affects the size of the dendritic arbor of PCs and the thickness of the molecular layer, it probably also causes a reduction in the number of granule cells. This probably results in reduced PF input to PCs. Changes in the thickness of the molecular and granular cell layers were accompanied by a significant weight reduction of the cerebellum ($P < 0.0001$) and by a significant decrease in the proportion of cerebellar to whole-brain weights ($P = 0.029$) of adult *lethargic* mice compared to wildtype (Fig. 3K and J), indicative of widespread effects of β_4 loss on brain development.

Lack of the calcium channel β_4 subunit impairs the development of high PC pacemaker frequency but not of firing regularity

Finding that the lack of β_4 in *lethargic* mice specifically reduces the PF input and dendritic morphology of cerebellar PCs, we reasoned that this might impair the output of these neurons. Therefore, spontaneous PC pacemaker activity was recorded in acute cerebellar slices from young and adult mice. At P15, locomotion is acquired and the cerebellar network is not fully developed (Altman, 1972). At 1 month of age, locomotion and the cerebellar networks are mature. Figure 4A shows tonic action potential firing of young and adult PCs from cell-attached recordings in acute cerebellar slices of wildtype and *lethargic* mice. Firing occurred at relatively low frequencies in young mice (P14–15) of both genotypes

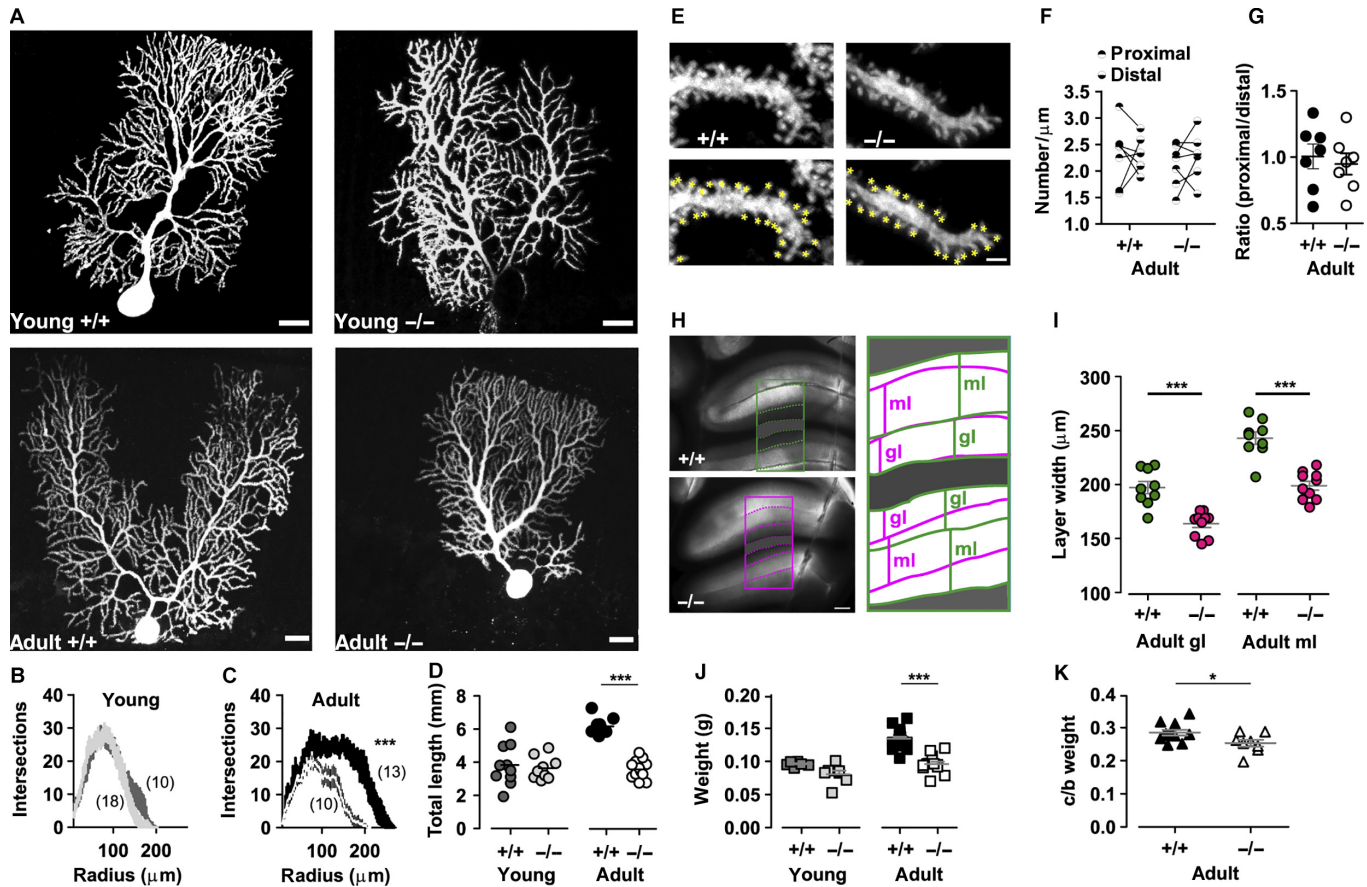


Fig. 3. Morphological analysis of Purkinje neurons, granular and molecular layers. (A) Purkinje neurons of juvenile and adult wildtype (+/+) and *lethargic* (-/-) mice, perfused with biocytin during patch-clamp recording and subsequently fluorescently labelled and analysed with confocal microscopy. Scale bars = 20 μ m. (B, C) Graphs of the number of radial intersections of dendrites at increasing distance from the soma (Scholl analysis) in young (B) and adult (C) +/+ and -/- mice. Note the significantly diminished branching of adult -/- PCs. (D) Total dendritic length is significantly increased in dendrites in adult +/+ PCs. (E) High-magnification images of PC dendrite segments in +/+ and -/- mice with dendritic spines highlighted by yellow marks (lower panels). Scale bar = 1.5 μ m. (F) Average spine density in proximal and distal dendritic segments in adult +/+ and -/- neurons; paired measurements in each cell are connected by lines. (G) Ratio between proximal and distal spine density. (H) Brightfield images of acute cerebellar slices from adult +/+ and -/- mice. Scale bar = 250 μ m. Masks outlining the granular and molecular layers are expanded and superimposed in the right panel. (I) Average width of adult +/+ and adult -/- granular and molecular layers. Note that both granular and molecular layers are significantly narrower in the cerebellar cortex of -/- mice. (J) Cerebellar weight of young +/+ (dark grey) and young -/- (light grey), adult +/+ (black) and adult -/- (white) mice. (K) Ratio between cerebellum and brain weight (c/b) in adult +/+ (black) and adult -/- (white) mice. Differences between multiple populations were analysed with one-way ANOVA followed by Bonferroni post-test (D, F, J, I). A Mann-Whitney test was used in the comparison between adult cerebellum/brain weight ratio and proximal/distal spine ratio (G, K). * $P < 0.05$, *** $P < 0.0001$.

(+/+, 50 ± 5 Hz; -/-, to 47 ± 5 Hz; $P = 0.7$; Fig. 4B). Firing frequencies increased to 97 ± 10 Hz in wildtype adults (P35–60). However, in adult *lethargic* mice PC firing frequencies failed to increase (38 ± 5 Hz; Fig. 4A and B) and were equal to values measured in the young animals. Accordingly, the age-related increase in firing frequency was highly significant only in the wildtype mouse cerebellum ($P = 0.002$), but not in the *lethargic* mouse cerebellum ($P = 0.2$). Furthermore, the firing frequency of wildtype adults was significantly higher than that of *lethargic* adults ($P < 0.0001$). Thus, in the absence of β_4 , functional maturation of the PC pacemaker firing frequency fails after P15. As Purkinje axons are the only cortical efferent, low PC firing rates correspond to decreased cerebellar cortical output.

To also quantify the regularity of PC action potential firing in *lethargic* and wildtype mice, we calculated the coefficient of variation (CV) of the inter-spike intervals (Fig. 4C). In young neurons CV was increased from 0.13 ± 0.01 in $\beta_4^{+/+}$ to 0.28 ± 0.07 in $\beta_4^{-/-}$ neurons ($P = 0.007$, unpaired t -test). However, after a

Bonferroni post-test, the difference between CV of young mice or between CV of adult mice was no longer significant (Table 3). In adults, the firing regularity had improved in both wildtype and *lethargic* mouse neurons (+/+, $P = 0.02$; -/-, $P = 0.008$; unpaired t -test); the difference in CV between the two genotypes was not statistically significant (0.09 ± 0.01 and 0.16 ± 0.03 , respectively; $P = 0.2$). Together these analyses demonstrate that in adult *lethargic* cerebellum the firing rate of PCs is substantially reduced without a concomitant loss of firing regularity. In wildtype and *lethargic* mice we observed tonic firing, bursting and silent PCs. In young and in adult wildtype mice, the tonic firing PCs accounted for 65% and silent PCs for 20% of the whole cell population. In *lethargic* mice, tonic firing was instead limited to 45% of the young and 37% of the adult PC cell population. This was coincident with an increased number of silent PCs to 45 and 50% in young and adult *lethargic* mice, respectively. In conclusion, not only were the tonic firing rates reduced but also the number of active neurons was diminished by the loss of β_4 , which could

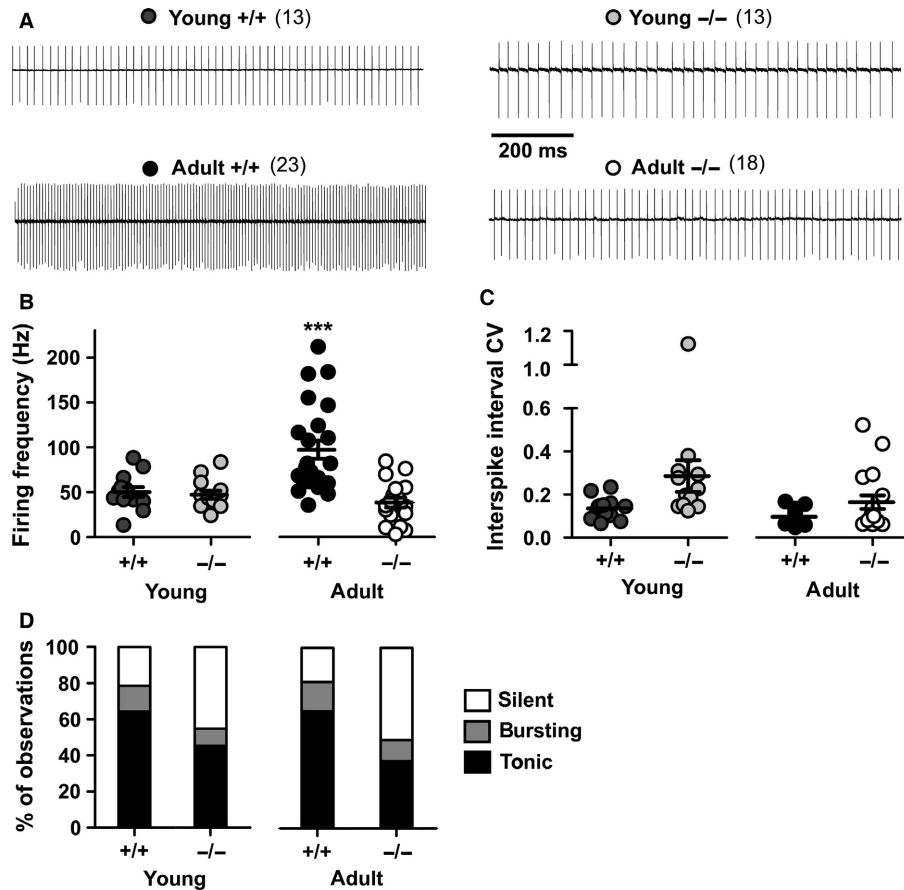


FIG. 4. Pacemaker firing of Purkinje neurons in young and adult wildtype (+/+) and *lethargic* (-/-) mice. (A) Representative cell-attached recordings; vertical deflection of baseline represents individual action potentials. (B, C) Average pacemaker firing frequency (B) and coefficient of variation of the inter-spike interval (C) in young and adult +/+ and -/- PCs. Each mark in the scatter plots represents individual average firing properties. Bars indicate mean \pm SEM. Note that the frequency of adult wildtype mice is significantly higher than that of *lethargic* mice. (D) Bar graph indicating the probability and the proportion between independent observations of silent, bursting and tonic firing cells in young and adult +/+ and -/- mice. Differences between firing frequencies were analysed with one-way ANOVA followed by Bonferroni post-test and differences between CV (not normally distributed) were analysed with Kruskal–Wallis test, followed by Dunn’s post-test. *** $P < 0.0001$. Numbers of independent samples are indicated in parentheses in the figure.

contribute to depression of cortical output. The burst firing mode occurred rarely and the proportion of bursting neurons in wildtype and *lethargic* mice (10–15% of the total cell population) was virtually the same at any age.

High pacemaker firing rates are not dependent on tonic glutamatergic neurotransmission

To examine whether the decreased PC tonic firing rates might be related to the observed reduction of PF–PC, we recorded spontaneous firing of PCs in cerebellar slices of wildtype and *lethargic* mice upon block of tonic neurotransmission (Fig. 5A). We used bath application of DNQX and gabazine, DNQX and AP-5, or DNQX and *trans*-ACPD for 15–60 min to block α -amino-3-hydroxy-5-methyl-4-isoxazolepropionic acid (AMPA), *N*-methyl-D-aspartate (NMDA), gamma-aminobutyric acid (GABA)_A and metabotropic glutamate receptors. However, none of these conditions affected the firing rates or firing regularity of PCs in wildtype (Fig. 5B, Table 4) or *lethargic* cerebellum. Thus, altered synaptic input is probably not involved in the short- to medium-term modulation of PC pacemaker firing frequency and therefore unlikely to be the cause for the differences in firing frequency observed in adult wildtype and *lethargic* mice. However, these experiments do not exclude possible long-term effects of altered neurotransmission

TABLE 3. Pacemaker firing frequency and coefficient of variation

	Frequency (Hz)	CV	<i>n</i>
+/+ young (P14–15)	50 \pm 5	0.135 \pm 0.014	13
-/- young (P14–15)	47 \pm 5	0.285 \pm 0.073	13
<i>P</i>	0.7*	0.007 [†]	
+/+ adult (P35–60)	97 \pm 10	0.096 \pm 0.006	23
-/- adult (P35–60)	38 \pm 5	0.164 \pm 0.031	18
<i>P</i>	< 0.0001*	0.2 [†]	
<i>P</i> young vs. adult +/+	0.002*	0.02 [†]	
<i>P</i> young vs. adult -/-	0.2*	0.008 [†]	
Multiple comparison (one-way ANOVA = * or K-W = [†]) <i>F</i> ; <i>P</i>	13.05*; < 0.0001	21.6 < 0.0001 [†]	
<i>Post-hoc</i> (young +/+ vs. -/-)	ns*	ns [†]	
<i>Post-hoc</i> (adult +/+ vs. -/-)	< 0.0001*	ns [†]	
<i>Post-hoc</i> (young +/+ vs. adult +/+)	< 0.01*	ns [†]	
<i>Post-hoc</i> test (young -/- vs. adult -/-)	ns*	<i>P</i> < 0.5 [†]	

Mean \pm SEM are reported. *P* (*) values refer to unpaired *t*-test. Multiple comparison refers to one-way ANOVA (*P*; *F*) and Bonferroni post-test. The coefficient of variation (CV) of -/- populations was not normally distributed, and therefore significance was tested with Mann–Whitney test and Kruskal–Wallis test (K-W statistic; *P*) followed by Dunn’s multiple comparison test ([†]). ns, not significant; -, not tested.

in *lethargic* mice and a critical involvement of β_4 in other potential modulatory pathways.

Afterhyperpolarization is not affected by the loss of β_4

Reduction of PC pacemaker rates occurs in an ataxia mutation of the BK calcium-activated potassium channel (Sausbier *et al.*, 2004). This is associated with a prominent decrease in potassium currents during afterhyperpolarization (AHP). If sparser pacemaker firing in *lethargic* PCs involved BK potassium currents, this would be revealed by smaller AHP amplitudes. However, whole cell recordings from regularly firing wildtype or *lethargic* neurons showed normal AHP with negative peaks of -56.6 ± 0.7 and -55.0 ± 1.9 mV, respectively (Fig. 6; $P = 0.4$). Furthermore, longer inter-spike intervals among our samples were not necessarily associated with smaller AHP. Therefore, small AHP derived from loss of BK potassium currents does not contribute to the *lethargic* phenotype.

Discussion

Loss of the calcium channel β_4 subunit causes motor impairment (Khan & Jinnah, 2002) with striking similarities between the *lethargic* ($\beta_4^{-/-}$) mouse and mouse models with $\text{Ca}_v2.1$ -related forms of ataxia (Fletcher *et al.*, 1996; Burgess & Noebels, 1999a,b; Barclay *et al.*, 2001; Guida *et al.*, 2001; Pietrobon, 2002). However, past investigations of physiological and pathophysiological roles of β_4 in the brain yielded conflicting results. Depending on the brain region or experimental system used β_4 was found either to be essential for

TABLE 4. Pacemaker firing frequency and coefficient of variation after pharmacological blockage of glutamate and/or GABA receptors; see also Fig. 5

	Frequency (Hz)	CV	<i>P</i>	<i>n</i>
$+/+$ DNQX/gbz	105 \pm 12	0.098 \pm 0.022	0.3; 0.9	4
$+/+$ DNQX/AP-5	74 \pm 9	0.128 \pm 0.021	0.15; 0.4	12
$+/+$ <i>trans</i> -ACPD	102 \pm 10	0.120 \pm 0.019	0.2; 0.5	11

Average \pm SEM are reported. *P* values refer to unpaired *t*-test. These experiments were carried out in adult mice (P35–60).

normal neuronal function (Caddick *et al.*, 1999; Lin *et al.*, 1999; Wittemann *et al.*, 2000), potentially relevant (McEnery *et al.*, 1998), or even entirely redundant with other β isoforms (Burgess *et al.*, 1999). Apparently the context of the brain region and the specific neuronal network is critical for understanding the role of the β_4 subunit in the etiology of the *lethargic* phenotype (Caddick *et al.*, 1999). Because of the importance of the cerebellar cortex in motor control we examined here (i) whether the loss of β_4 recapitulates the effects of loss of $\text{Ca}_v2.1$ on cerebellar function and morphology, (ii) which functions of PC networks are primarily impaired by the loss of β_4 and (iii) how this may contribute to the ataxic phenotype in *lethargic* mice. The present slice electrophysiology study demonstrates that the lack of the calcium channel β_4 subunit causes a decreased late development in cerebellar cortical networks, characterized by reduced PF–PC input, shorter PC dendrites and depressed PC output (Fig. 7). This is the first study addressing the physiological role of β_4 and its involvement in the etiology of ataxia in the context of native PC networks in acute cerebellar slices.

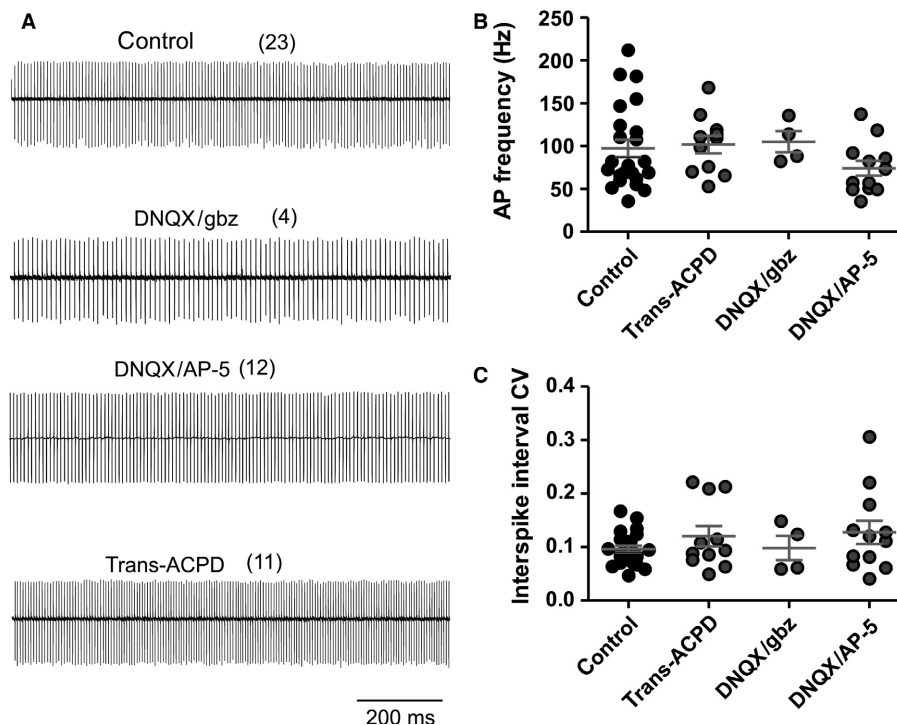


FIG. 5. Pacemaker firing of wildtype adult Purkinje neurons in control conditions and after blockage of fast synaptic neurotransmission. (A) Representative cell-attached recording from PCs in untreated control slices, and in the presence of: 10 μM 6,7 dinitroquinoxaline-2,3-dione and 10 μM SR 95531 (DNQX/gbz); 10 μM DNQX and 50 μM AP-5 (DNQX/AP-5); or 50 μM *trans*-ACPD. (B, C) Average pacemaker firing frequency (B) and coefficient of variation of the interspike interval (C) in untreated neurons and after pharmacological treatment. Differences between action potential firing in the presence of drugs and untreated controls were analysed with unpaired *t*-test for normally distributed samples (frequencies) or Mann–Whitney test for non-normally distributed samples (CV). Numbers of independent samples are indicated in parentheses in the figure.

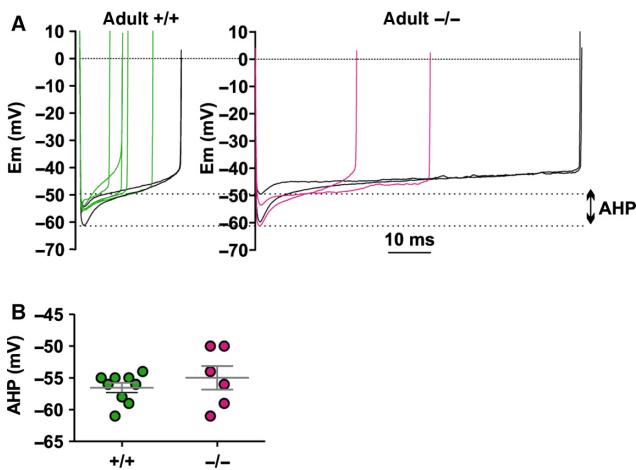


FIG. 6. Whole-cell current clamp recordings of afterhyperpolarizations (AHPs) in adult PCs. (A) Representative action potential inter-spikes from regularly firing cells in adult wildtype (+/+) and *lethargic* (-/-) mice; dotted lines indicate the range of AHP. Note that action potentials with the same inter-spike duration produce extremely different amplitudes of AHP (highlighted in black). (B) Scatter plot of average AHP in +/+ and -/- pacemaker firing neurons. Each mark represents an individual average AHP. Differences between AHP were analysed with unpaired *t*-test.

Does loss of the β_4 subunit affect known functions of $Ca_v2.1$ in the cerebellum?

Because the β_4 subunit is the primary partner of $Ca_v2.1$ in cerebellum and loss-of-function mutations of both calcium channel subunits result in ataxia (Burgess *et al.*, 1997; Burgess & Noebels, 1999a; Escayg *et al.*, 2000; Guida *et al.*, 2001; Pietrobon, 2002; Buraei & Yang, 2010; Schlick *et al.*, 2010), it is reasonable to expect that loss of either one of these proteins affects the same brain functions. Indeed, the loss of β_4 in the *lethargic* mouse recapitulates a number of impairments of cerebellar function and morphology previously observed in the ataxic $Ca_v2.1$ mouse models *rocker*, *tottering* and *purky* (Zwingman *et al.*, 2001; Matsushita *et al.*, 2002; Kodama *et al.*, 2006; Erickson *et al.*, 2007; Mark *et al.*, 2011). These common impairments encompass a retarded cerebellar development, smaller PC dendrites, PF depression, the resulting imbalance between PF and CF input to PCs, and the late onset of the disease phenotype. Moreover, both the *lethargic* and the *rocker* mice show a normal synaptic density in PC dendrites (Kodama *et al.*, 2006), although this was not observed in several other ataxic models (Kashiwabuchi *et al.*, 1995; Kurihara *et al.*, 1997; Oda *et al.*, 2011). This similarity indicates that altered function of cerebellar P/Q-type calcium channels may contribute to the *lethargic* phenotype. Importantly, it further demonstrates that β_4 is not functionally redundant, as its loss cannot be fully compensated for by other β isoforms.

On the other hand, other cerebellar functions are differently affected by the loss of $Ca_v2.1$ and β_4 . For example general presynaptic loss of $Ca_v2.1$ affects the spontaneous synaptic activity (Lonchamp *et al.*, 2009; Galliano *et al.*, 2013) and alters release probability (Maejima *et al.*, 2013). However, in the *lethargic* mouse cerebellum we found that spontaneous synaptic activity and PPF of PF-PC PSCs were not reduced. In theory, the lack of a presynaptic phenotype might indicate compensation for the lost β_4 function in PF-PC synapses. However, only complete knockout of $Ca_v2.1$ in cerebellar granule cells affected presynaptic PF-PC function (Lonchamp *et al.*, 2009; Galliano *et al.*, 2013; Maejima *et al.*, 2013), whereas partial loss of $Ca_v2.1$ function did not show a presynaptic phenotype (Matsushita *et al.*, 2002; Kodama *et al.*, 2006). Apparently the safety margin with regard to

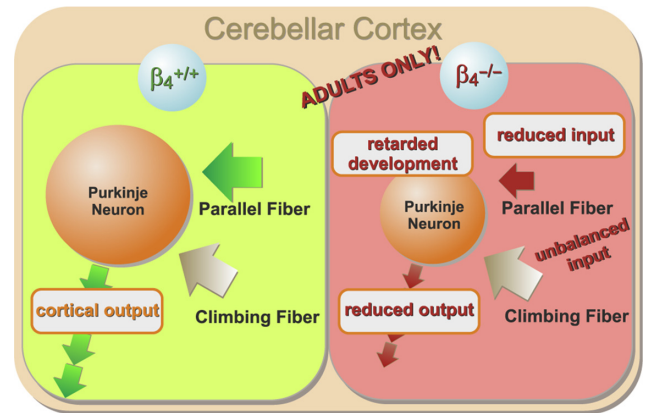


FIG. 7. Changes in cerebellar cortical network caused by the lack of β_4 in adult *lethargic* mice. In the absence of β_4 the input from PFs is reduced, whereas the input from CFs is spared. Thus, the PC inputs are unbalanced. The size of PCs (dendritic branching) and the width of the granular cell layer are reduced. The firing frequency of PCs and thus cerebellar output is reduced. All these deficits affect only adult and not juvenile *lethargic* mice, consistent with a developmental retardation of cerebellar cortical networks in *lethargic* mice.

calcium influx in this synapse is very high (Matsushita *et al.*, 2002), so that a possibly small reduction of P/Q-type channels caused by the lack of β_4 may have no functional consequence. By contrast, the spontaneous ePSC amplitude in juvenile *lethargic* mice was increased. While this together with unaltered PPR does not suggest impairment of presynaptic P/Q-type channels, the slight increase in the *lethargic* PSC amplitude may relate to more subtle changes in the formation of presynaptic channel complexes (Iwasaki *et al.*, 2000) upon loss of β_4 . The situation in the cerebellum is probably different from that in other brain regions as the loss of β_4 resulted in reduced presynaptic function in cultured hippocampal neurons (Wittemann *et al.*, 2000; Xie *et al.*, 2007), as well as in whole-brain synaptosome preparations (Lin *et al.*, 1999). Moreover, even though the PF PSC was decreased in the absence of β_4 , the unaltered PF PPR and the presence of all-or-none CF responses suggest that unlike $Ca_v2.1^{-/-}$, $\beta_4^{-/-}$ has little relevance for heterosynaptic competition between PFs and CFs or for homosynaptic competition among CFs (Miyazaki *et al.*, 2004).

Notably, the effects of the loss of β_4 in *lethargic* mice were not limited to deficiencies of cerebellar functions previously observed in $Ca_v2.1$ mutants. We also observed a dramatically decreased PC pacemaker frequency, while the regularity of pacemaker firing was maintained. A similar deficiency of PC pacemaker activity was not observed upon $Ca_v2.1$ mutation (*leaner*) nor in closely related (*ducky*) forms of ataxia where both controls and mutants had average firing rates between 75 and 115 Hz (Sausbier *et al.*, 2004; Walter *et al.*, 2006). In contrast, *lethargic* PCs had firing rates of about 40 Hz, which is significantly reduced compared to wildtype controls which fired at about 100 Hz. In *lethargic* mice, the β_4 -specific dysfunction of PC firing suggests a critical function of this protein in the context of another type of calcium channel that cannot be compensated for by alternative β isoforms (McEnery *et al.*, 1998; Burgess *et al.*, 1999). Alternatively, reduced cerebellar PC firing rates as well as lower number of constitutively active neurons could result from a loss of calcium-activated BK potassium currents (Sausbier *et al.*, 2004). However, in $\beta_4^{-/-}$ mice, AHP was not affected. Even so, prolonged inter-spike intervals and reduced cortical output may contribute to the motor impairment of *lethargic* as well as of $BK^{-/-}$ mice.

Overall, this study reveals both common and specific functions of β_4 and $Ca_v2.1$ in cerebellar networks. Considering the role of β_4 as

an auxiliary calcium channel subunit, the common deficiencies involving PF–PC PSCs and PC development suggest a role of the β_4 isoform in modulating PSCs, pacemaker activity and dendritic maturation. In contrast, the absence of a phenotype in CF–PC synapse function and in PF–PC release probability indicates that for neurotransmitter release and synaptic competition β subunit functions may be redundant. Furthermore, the absence of β_4 -specific defects of PC pacemaker firing regularity confirms an earlier study showing the redundancy of β_4 at the PC soma (Burgess *et al.*, 1999). Conversely, β_4 -specific defects of PC pacemaker frequency suggest an essential function of β_4 with a hitherto unidentified calcium channel isoform other than $\text{Ca}_v2.1$. Finally, considering the role of β_{4b} as a regulator of gene transcription (Etemad *et al.*, 2014), it is possible that loss of β_4 may affect cerebellar development through calcium channel-independent pathways. Taken together, the similarities and differences between $\beta_4^{-/-}$ and $\text{Ca}_v2.1$ mutants suggests that $\text{Ca}_v2.1$ -related and unrelated dysfunctions may coexist in the *lethargic* cerebellum.

How does the loss of β_4 affect the network activity in the cerebellar cortex of *lethargic* mice?

The observed reduction of the evoked PF input in cerebellar PCs is one of the most striking functional consequences of the loss of β_4 . In *lethargic* mice the cerebellar granular layer was thinner. This may imply a reduced number of granule cells and consequently fewer PFs. More importantly, the distal dendritic arbor of PCs in *lethargic* mice had a reduced height and width and with slightly sparser branching (Fig. 3; Fig. S1). According to our experimental paradigm, electrical stimulation of a given PF bundle would recruit a smaller dendritic area of *lethargic* PCs than in controls. This contributes to limiting the evoked PF–PC PSCs in *lethargic* mice. However, given the unchanged synaptic density (Fig. 3) and only mildly reduced distal dendritic density (Fig. S1) the morphological changes cannot fully account for the large reduction in the PF–PC PSC recorded in *lethargic* mice.

This explanation for the reduced PF volley is also challenged by previous research suggesting that other presynaptic and postsynaptic factors might contribute to aberrant neurotransmission upon loss of $\text{Ca}_v2.1$ or β_4 (Caddick *et al.*, 1999; Lin *et al.*, 1999; Wittemann *et al.*, 2000; Kodama *et al.*, 2006; Xie *et al.*, 2007). However, in contrast to defects of neurotransmission found in $\text{Ca}_v2.1$ -related pathologies (Pietrobon, 2002, 2005) and to what was observed upon loss of β_4 in other neuronal systems (Lin *et al.*, 1999; Wittemann *et al.*, 2000; Xie *et al.*, 2007), we found unaltered PF–PC release probability, suggesting that the loss of β_4 in cerebellum did not severely affect presynaptic neurotransmitter release. This along with unaltered spine density of PF–PC synapses suggests a normal presynaptic physiology in the cerebellum of *lethargic* mice. The decreased PF–PC PSC could therefore be caused by specific impairment of postsynaptic function (Kodama *et al.*, 2006) or directly related to the reduced distal branching of PC dendrites. Given the abundance of $\text{Ca}_v2.1$ channels in PC dendrites and their function in the amplification of postsynaptic currents (De Schutter & Bower, 1994), a potential reduction of dendritic $\text{Ca}_v2.1$ is expected to alter processing of the PF input. As postsynaptic enrichment of $\text{Ca}_v2.1$ channels is an age-dependent phenomenon and follows a somatodendritic gradient (Indriati *et al.*, 2013), a loss of postsynaptic $\text{Ca}_v2.1$ would well agree with the observed reduction of distal dendritic tree (Fig. S1), the decreased PF–PC input and the late onset of the *lethargic* phenotype. Specifically, dendritic spikes (Llinas *et al.*, 1968; Llinas & Sugimori, 1980) may be affected by the postsynaptic

loss of $\text{Ca}_v2.1$ (Tank *et al.*, 1988) in *lethargic* mice, which in turn would impair the processing and integration of PF and CF inputs (Rancz & Hausser, 2006; Davie *et al.*, 2008), and long- and short-term synaptic plasticity (Kreitzer & Regehr, 2001; Golding *et al.*, 2002; Holthoff *et al.*, 2004; Rancz & Hausser, 2006).

A reduced PC firing rate in adult *lethargic* mice was another striking effect of the loss of the β_4 subunit in cerebellar cortex. Because PF and CF input have antagonistic effects on PC excitability and pacemaker rates (Shibuki & Kimura, 1997; Smith & Otis, 2003; Cerminara & Rawson, 2004), the skewed proportion between PFs and CFs observed here in *lethargic* mice might dictate reduced rates of pacemaker firing in PCs. However, PC firing frequency was not affected by the acute block of tonic neurotransmission, thus questioning a causal link between reduced PF input and reduced PC pacemaker activity in the *lethargic* cerebellum.

How do defects in the cerebellar network contribute to the motor impairment in *lethargic* mice?

Our slice electrophysiology analysis of the cerebellar network in *lethargic* mice revealed deficiencies at the input and output side of PCs, both of which could contribute to ataxia. Motor learning relies on the plasticity of PCs and their role in integrating the inputs from PFs and CFs (Ito *et al.*, 1982; Hansel & Linden, 2000; Ito, 2001). In *lethargic* mice evoked PF PSCs are specifically reduced, which could impair motor learning (Galliano *et al.*, 2013). In the presynaptic compartment this could be caused by a paucity of granule cells from which the PFs originate, and in the postsynaptic compartment by smaller medial and distal PC dendrites onto which PFs project. Yet, the CF input and proximal PC dendrites are unaffected by the loss of β_4 . The resulting imbalance between PF and CF input onto PCs by itself could account for impaired plasticity, learning and coordination (Ito *et al.*, 1982; Hansel & Linden, 2000; Ito, 2001; Galliano *et al.*, 2013). Similarly, defective dendritic processing of both PF and CF inputs could lead to impaired network plasticity (Kreitzer & Regehr, 2001; Golding *et al.*, 2002; Holthoff *et al.*, 2004; Rancz & Hausser, 2006). Ultimately, cerebellar dysfunctions must be reflected in altered PC tonic output. As PCs represent the sole cerebellar cortical output, the observed slowed PC pacemaker firing will result in inefficient inhibition of the deep cerebellar nuclei (Gauck & Jaeger, 2000). Similarly reduced tonic output has previously been described in other mouse models with impaired motor coordination (Sausbier *et al.*, 2004). Thus, reduced tonic firing of cerebellar PCs could be a major cause of the motor impairment generated by the loss of the calcium channel β_4 subunit in *lethargic* mice.

Conflict of interest

The authors declare no competing financial interests.

Supporting Information

Additional supporting information can be found in the online version of this article:

Fig. S1. Substantially reduced size and modestly reduced density of the distal dendritic arbor in *lethargic* Purkinje neurons.

Acknowledgements

We thank Drs J. Striessnig, A. Lieb and G. Obermair for practical support and valuable scientific discussion, Dr M. Offerdinger for valuable support in

the Biooptic facility of the Medical University of Innsbruck and Dr E. Meijering, Biomedical Imaging Group, Erasmus University Medical Center Rotterdam, for providing the image analysis plugin 'Neuron J'. This work was supported by the Austrian Science Fund (FWF) grants F44010 (SFB-F44 – Cell Signaling in chronic CNS disorders), F44060, P23479 and P27031 (to B.E.F.), the Medical University Innsbruck (ST712600S441) and the Tiroler Wissenschaftsfond 2013 (UNI-0404/1419 to B.B.).

Abbreviations

ACPD, 1-amino-1,3-dicarboxycyclopentane; AHP, afterhyperpolarization; Cav, voltage-activated calcium channel; CF, climbing fibre; CNS, central nervous system; CV, coefficient of variation; ePSC, excitatory postsynaptic current; iPSC, inhibitory postsynaptic current; PC, Purkinje cell; PF, parallel fibre; PPF, paired pulse facilitation; PPR, paired pulse ratio.

References

- Altman, J. (1972) Postnatal development of the cerebellar cortex in the rat. I. The external germinal layer and the transitional molecular layer. *J. Comp. Neurol.*, **145**, 353–397.
- Barclay, J., Balaguero, N., Mione, M., Ackerman, S.L., Letts, V.A., Brodbeck, J., Canti, C., Meir, A. *et al.* (2001) Ducky mouse phenotype of epilepsy and ataxia is associated with mutations in the *Cacna2d2* gene and decreased calcium channel current in cerebellar Purkinje cells. *J. Neurosci.*, **21**, 6095–6104.
- Benedetti, B., Matyash, V. & Kettenmann, H. (2011) Astrocytes control GABAergic inhibition of neurons in the mouse barrel cortex. *J. Physiol.*, **589**, 1159–1172.
- Brodbeck, J., Davies, A., Courtney, J.M., Meir, A., Balaguero, N., Canti, C., Moss, F.J., Page, K.M. *et al.* (2002) The *duffy* mutation in *Cacna2d2* results in altered Purkinje cell morphology and is associated with the expression of a truncated alpha 2 delta-2 protein with abnormal function. *J. Biol. Chem.*, **277**, 7684–7693.
- Buraei, Z. & Yang, J. (2010) The b subunit of voltage-gated Ca^{2+} channels. *Physiol. Rev.*, **90**, 1461–1506.
- Burgess, D.L. & Noebels, J.L. (1999a) Single gene defects in mice: the role of voltage-dependent calcium channels in absence models. *Epilepsy Res.*, **36**, 111–122.
- Burgess, D.L. & Noebels, J.L. (1999b) Voltage-dependent calcium channel mutations in neurological disease. *Ann. N.Y. Acad. Sci.*, **868**, 199–212.
- Burgess, D.L., Jones, J.M., Meisler, M.H. & Noebels, J.L. (1997) Mutation of the Ca^{2+} channel beta subunit gene *Chb4* is associated with ataxia and seizures in the *lethargic (lh)* mouse. *Cell*, **88**, 385–392.
- Burgess, D.L., Biddlecome, G.H., McDonough, S.I., Diaz, M.E., Zilinski, C.A., Bean, B.P., Campbell, K.P. & Noebels, J.L. (1999) Beta subunit reshuffling modifies N- and P/Q-type Ca^{2+} channel subunit compositions in lethargic mouse brain. *Mol. Cell Neurosci.*, **13**, 293–311.
- Caddick, S.J., Wang, C., Fletcher, C.F., Jenkins, N.A., Copeland, N.G. & Hosford, D.A. (1999) Excitatory but not inhibitory synaptic transmission is reduced in lethargic (*Cacnb4^{lh}*) and tottering (*Cacna1atg*) mouse thalami. *J. Neurophysiol.*, **81**, 2066–2074.
- Campiglio, M. & Flucher, B.E. (2015) The role of auxiliary subunits for the functional diversity of voltage-gated calcium channels. *J. Cell. Physiol.*, **230**, 2019–2031.
- Cerminara, N.L. & Rawson, J.A. (2004) Evidence that climbing fibers control an intrinsic spike generator in cerebellar Purkinje cells. *J. Neurosci.*, **24**, 4510–4517.
- Davie, J.T., Clark, B.A. & Hausser, M. (2008) The origin of the complex spike in cerebellar Purkinje cells. *J. Neurosci.*, **28**, 7599–7609.
- De Schutter, E. & Bower, J.M. (1994) Simulated responses of cerebellar Purkinje cells are independent of the dendritic location of granule cell synaptic inputs. *Proc. Natl. Acad. Sci. USA*, **91**, 4736–4740.
- Dolphin, A.C. (2012) Calcium channel auxiliary alpha2delta and beta subunits: trafficking and one step beyond. *Nat. Rev. Neurosci.*, **13**, 542–555.
- Dung, H.C. & Swigart, R.H. (1971) Experimental studies of 'lethargic' mutant mice. *Tex. Rep. Biol. Med.*, **29**, 273–288.
- Erickson, M.A., Haburcak, M., Smukler, L. & Dunlap, K. (2007) Altered functional expression of Purkinje cell calcium channels precedes motor dysfunction in tottering mice. *Neuroscience*, **150**, 547–555.
- Escayg, A., De Waard, M., Lee, D.D., Bichet, D., Wolf, P., Mayer, T., Johnston, J., Baloh, R. *et al.* (2000) Coding and noncoding variation of the human calcium-channel beta4-subunit gene *CACNB4* in patients with idiopathic generalized epilepsy and episodic ataxia. *Am. J. Hum. Genet.*, **66**, 1531–1539.
- Etemad, S., Obermair, G.J., Bindreither, D., Benedetti, A., Stanika, R., Di Biase, V., Burtcher, V., Koschak, A. *et al.* (2014) Differential neuronal targeting of a new and two known calcium channel beta4 subunit splice variants correlates with their regulation of gene expression. *J. Neurosci.*, **34**, 1446–1461.
- Fletcher, C.F., Lutz, C.M., O'Sullivan, T.N., Shaughnessy, J.D. Jr, Hawkes, R., Frankel, W.N., Copeland, N.G. & Jenkins, N.A. (1996) Absence epilepsy in tottering mutant mice is associated with calcium channel defects. *Cell*, **87**, 607–617.
- Galliano, E., Gao, Z., Schonewille, M., Todorov, B., Simons, E., Pop, A.S., D'Angelo, E., van den Maagdenberg, A.M. *et al.* (2013) Silencing the majority of cerebellar granule cells uncovers their essential role in motor learning and consolidation. *Cell Rep.*, **3**, 1239–1251.
- Gauk, V. & Jaeger, D. (2000) The control of rate and timing of spikes in the deep cerebellar nuclei by inhibition. *J. Neurosci.*, **20**, 3006–3016.
- Golding, N.L., Staff, N.P. & Spruston, N. (2002) Dendritic spikes as a mechanism for cooperative long-term potentiation. *Nature*, **418**, 326–331.
- Guida, S., Trettel, F., Pagnutti, S., Mantuano, E., Tottene, A., Veneziano, L., Fellin, T., Spadaro, M. *et al.* (2001) Complete loss of P/Q calcium channel activity caused by a *CACNA1A* missense mutation carried by patients with episodic ataxia type 2. *Am. J. Hum. Genet.*, **68**, 759–764.
- Hamann, M., Rossi, D.J. & Attwell, D. (2002) Tonic and spillover inhibition of granule cells control information flow through cerebellar cortex. *Neuron*, **33**, 625–633.
- Hansel, C. & Linden, D.J. (2000) Long-term depression of the cerebellar climbing fiber–Purkinje neuron synapse. *Neuron*, **26**, 473–482.
- Holthoff, K., Kovalchuk, Y., Yuste, R. & Konnerth, A. (2004) Single-shock LTD by local dendritic spikes in pyramidal neurons of mouse visual cortex. *J. Physiol.*, **560**, 27–36.
- Indriati, D.W., Kamasawa, N., Matsui, K., Meredith, A.L., Watanabe, M. & Shigemoto, R. (2013) Quantitative localization of Cav2.1 (P/Q-type) voltage-dependent calcium channels in Purkinje cells: somatodendritic gradient and distinct somatic co-clustering with calcium-activated potassium channels. *J. Neurosci.*, **33**, 3668–3678.
- Ito, M. (2001) Cerebellar long-term depression: characterization, signal transduction, and functional roles. *Physiol. Rev.*, **81**, 1143–1195.
- Ito, M., Sakurai, M. & Tongroach, P. (1982) Climbing fibre induced depression of both mossy fibre responsiveness and glutamate sensitivity of cerebellar Purkinje cells. *J. Physiol.*, **324**, 113–134.
- Iwasaki, S., Momiyama, A., Uchitel, O.D. & Takahashi, T. (2000) Developmental changes in calcium channel types mediating central synaptic transmission. *J. Neurosci.*, **20**, 59–65.
- Kashiwabuchi, N., Ikeda, K., Araki, K., Hirano, T., Shibuki, K., Takayama, C., Inoue, Y., Kutsuwada, T. *et al.* (1995) Impairment of motor coordination, Purkinje cell synapse formation, and cerebellar long-term depression in GluR delta 2 mutant mice. *Cell*, **81**, 245–252.
- Khan, Z. & Jinnah, H.A. (2002) Paroxysmal dyskinesias in the lethargic mouse mutant. *J. Neurosci.*, **22**, 8193–8200.
- Kodama, T., Itsukaichi-Nishida, Y., Fukazawa, Y., Wakamori, M., Miyata, M., Molnar, E., Mori, Y., Shigemoto, R. *et al.* (2006) A Cav2.1 calcium channel mutation rocker reduces the number of postsynaptic AMPA receptors in parallel fiber–Purkinje cell synapses. *Eur. J. Neurosci.*, **24**, 2993–3007.
- Kreitzer, A.C. & Regehr, W.G. (2001) Retrograde inhibition of presynaptic calcium influx by endogenous cannabinoids at excitatory synapses onto Purkinje cells. *Neuron*, **29**, 717–727.
- Kurihara, H., Hashimoto, K., Kano, M., Takayama, C., Sakimura, K., Mishina, M., Inoue, Y. & Watanabe, M. (1997) Impaired parallel fiber→Purkinje cell synapse stabilization during cerebellar development of mutant mice lacking the glutamate receptor delta2 subunit. *J. Neurosci.*, **17**, 9613–9623.
- Lin, F., Barun, S., Lutz, C.M., Wang, Y. & Hosford, D.A. (1999) Decreased $^{45}\text{Ca}^{2+}$ uptake in P/Q-type calcium channels in homozygous lethargic (*Cacnb4^{lh}*) mice is associated with increased beta3 and decreased beta4 calcium channel subunit mRNA expression. *Brain Res. Mol. Brain Res.*, **71**, 1–10.
- Llinas, R. & Sugimori, M. (1980) Electrophysiological properties of in vitro Purkinje cell dendrites in mammalian cerebellar slices. *J. Physiol.*, **305**, 197–213.
- Llinas, R., Nicholson, C., Freeman, J.A. & Hillman, D.E. (1968) Dendritic spikes and their inhibition in alligator Purkinje cells. *Science*, **160**, 1132–1135.

- Lonchamp, E., Dupont, J.L., Doussau, F., Shin, H.S., Poulain, B. & Bossu, J.L. (2009) Deletion of Cav2.1($\alpha 1_A$) subunit of Ca^{2+} -channels impairs synaptic GABA and glutamate release in the mouse cerebellar cortex in cultured slices. *Eur. J. Neurosci.*, **30**, 2293–2307.
- Maejima, T., Wollenweber, P., Teusner, L.U., Noebels, J.L., Herlitze, S. & Mark, M.D. (2013) Postnatal loss of P/Q-type channels confined to rhombic-lip-derived neurons alters synaptic transmission at the parallel fiber to purkinje cell synapse and replicates genomic Cacna1a mutation phenotype of ataxia and seizures in mice. *J. Neurosci.*, **33**, 5162–5174.
- Mark, M.D., Maejima, T., Kuckelsberg, D., Yoo, J.W., Hyde, R.A., Shah, V., Gutierrez, D., Moreno, R.L. *et al.* (2011) Delayed postnatal loss of P/Q-type calcium channels recapitulates the absence epilepsy, dyskinesia, and ataxia phenotypes of genomic Cacna1a mutations. *J. Neurosci.*, **31**, 4311–4326.
- Matsushita, K., Wakamori, M., Rhyu, I.J., Arii, T., Oda, S., Mori, Y. & Imoto, K. (2002) Bidirectional alterations in cerebellar synaptic transmission of tottering and rolling Ca^{2+} channel mutant mice. *J. Neurosci.*, **22**, 4388–4398.
- McEnery, M.W., Copeland, T.D. & Vance, C.L. (1998) Altered expression and assembly of N-type calcium channel $\alpha 1B$ and β subunits in epileptic lethargic (*lh/lh*) mouse. *J. Biol. Chem.*, **273**, 21435–21438.
- Miyazaki, T., Hashimoto, K., Shin, H.S., Kano, M. & Watanabe, M. (2004) P/Q-type Ca^{2+} channel $\alpha 1A$ regulates synaptic competition on developing cerebellar Purkinje cells. *J. Neurosci.*, **24**, 1734–1743.
- Noebels, J.L. (2012) The voltage-gated calcium channel and absence epilepsy. In Noebels, J.L., Avoli, M., Rogawski, M.A., Olsen, R.W. & Delgado-Escueta, A.V. (Eds), *Jasper's Basic Mechanisms of the Epilepsies*. National Center for Biotechnology Information, Bethesda, MD, ISBN-10: 0199746540; ISBN-13: 978-0199746545; pp. 1–16.
- Obermair, G.J., Schlick, B., Di Biase, V., Subramanyam, P., Gebhart, M., Baumgartner, S. & Flucher, B.E. (2010) Reciprocal interactions regulate targeting of calcium channel β subunits and membrane expression of $\alpha 1A$ subunits in cultured hippocampal neurons. *J. Biol. Chem.*, **285**, 5776–5791.
- Oda, S.I., Lee, K.J., Arii, T., Imoto, K., Hyun, B.H., Park, I.S., Kim, H. & Rhyu, I.J. (2011) Differential regulation of Purkinje cell dendritic spines in rolling mouse Nagoya (*tg/tg*), P/Q type calcium channel ($\alpha 1_A/Ca_v2.1$) mutant. *Anat. Cell Biol.*, **43**, 211–217.
- Pietrobon, D. (2002) Calcium channels and channelopathies of the central nervous system. *Mol. Neurobiol.*, **25**, 31–50.
- Pietrobon, D. (2005) Function and dysfunction of synaptic calcium channels: insights from mouse models. *Curr. Opin. Neurobiol.*, **15**, 257–265.
- Rancz, E.A. & Hausser, M. (2006) Dendritic calcium spikes are tunable triggers of cannabinoid release and short-term synaptic plasticity in cerebellar Purkinje neurons. *J. Neurosci.*, **26**, 5428–5437.
- Sausbier, M., Hu, H., Arntz, C., Feil, S., Kamm, S., Adelsberger, H., Sausbier, U., Sailer, C.A. *et al.* (2004) Cerebellar ataxia and Purkinje cell dysfunction caused by Ca^{2+} -activated K^+ channel deficiency. *Proc. Natl. Acad. Sci. USA*, **101**, 9474–9478.
- Schlick, B., Flucher, B.E. & Obermair, G.J. (2010) Voltage-activated calcium channel expression profiles in mouse brain and cultured hippocampal neurons. *Neuroscience*, **167**, 786–798.
- Shibuki, K. & Kimura, S. (1997) Dynamic properties of nitric oxide release from parallel fibres in rat cerebellar slices. *J. Physiol.*, **498**(Pt 2), 443–452.
- Smith, S.L. & Otis, T.S. (2003) Persistent changes in spontaneous firing of Purkinje neurons triggered by the nitric oxide signaling cascade. *J. Neurosci.*, **23**, 367–372.
- Tadmouri, A., Kiyonaka, S., Barbado, M., Rousset, M., Fablet, K., Sawamura, S., Bahembera, E., Pernet-Gallay, K. *et al.* (2012) Cacnb4 directly couples electrical activity to gene expression, a process defective in juvenile epilepsy. *EMBO J.*, **31**, 3730–3744.
- Tank, D.W., Sugimori, M., Connor, J.A. & Llinas, R.R. (1988) Spatially resolved calcium dynamics of mammalian Purkinje cells in cerebellar slice. *Science*, **242**, 773–777.
- Walter, J.T., Alvina, K., Womack, M.D., Chevez, C. & Khodakhah, K. (2006) Decreases in the precision of Purkinje cell pacemaking cause cerebellar dysfunction and ataxia. *Nat. Neurosci.*, **9**, 389–397.
- Wittemann, S., Mark, M.D., Rettig, J. & Herlitze, S. (2000) Synaptic localization and presynaptic function of calcium channel $\beta 4$ -subunits in cultured hippocampal neurons. *J. Biol. Chem.*, **275**, 37807–37814.
- Xie, M., Li, X., Han, J., Vogt, D.L., Wittemann, S., Mark, M.D. & Herlitze, S. (2007) Facilitation versus depression in cultured hippocampal neurons determined by targeting of Ca^{2+} channel $Ca_v\beta_4$ versus $Ca_v\beta_2$ subunits to synaptic terminals. *J. Cell Biol.*, **178**, 489–502.
- Zwingman, T.A., Neumann, P.E., Noebels, J.L. & Herrup, K. (2001) Rocker is a new variant of the voltage-dependent calcium channel gene Cacna1a. *J. Neurosci.*, **21**, 1169–1178.